

## Different concepts for the coupling of porous-media flow with lower-dimensional pipe flow

M. O. Doğan<sup>1,2</sup>, H. Class<sup>2</sup> and R. Helmig<sup>2</sup>

**Abstract:** Many flow problems in environmental, technical and biological systems are characterized by a distinct interaction between a flow region in porous-medium and a free-flow region in quasi-one-dimensional hollow structures. In this study, different model concepts, based on a dual-continuum strategy, for the simulation of coupled porous-media flow and (lower-dimensional) pipe flow are further developed and tested. The dual-continuum concept is extended for coupling multi-phase porous-media flow with lower-dimensional single-phase free flow. The complexity of the considered flow regimes is increased gradually. Examples are given for a coupled single-phase incompressible and compressible flow in both porous-media and pipe flow domains. Furthermore, the coupling of single-phase pipe flow with a multi-phase flow based on Richard's equation for the unsaturated soil zone is modeled, where the important role of capillary effects for the mass exchange rate between the two continua could be illustrated. The last example introduces a concept for a two-phase porous-media flow coupled with a single-phase (gas) pipe-flow problem, which revealed that the mobility exchange term can be decisive for the mass exchange rate.

**Keywords:** porous-media flow, pipe flow, lower-dimensional coupling

### 1 Introduction

Numerical models for simulating flow and transport in porous media are applicable in many environmental, technical and biological problems. Distinct structures embedded in the porous media often make conceptual modeling difficult. In particular, if the porous medium is intersected with distinct quasi-one-dimensional hollow structures, porous-media flow and free flow in the hollow structures can interact strongly. In porous media, the velocities are calculated by using Darcy's Law

---

<sup>1</sup> Author for correspondence (E-mail: onur.dogan@iws.uni-stuttgart.de; Tel: 0049/711/68567014)

<sup>2</sup> Lehrstuhl für Hydromechanik und Hydrosystemmodellierung, Institut für Wasserbau, Universität Stuttgart, Pfaffenwaldring 61, 70569 Stuttgart, Germany

[Darcy (1856)], where the Reynold's number is typically less than unity. Generally, in free-flow regions Darcy's Law is not applicable.

Examples for such systems are:

- Mines: Methane released from unmined coal seams migrates through the porous rocks, but also through tunnels and shafts in the mine.
- Landslides: A sudden water infiltration through macropores may trigger landslides.
- Fuel cells: The supply of reactive gases through free-flow channels interacts strongly with the advective-diffusive transport through the porous diffusion layers to the reaction layers.
- Cancer therapy: Therapeutic agents are delivered via the blood vessels into tissue, targeting the tumor cells.

The general approaches to coupling porous-media flow with free-flow models may be divided into two main groups, (i) equi-dimensional coupling and (ii) lower-dimensional coupling. In equi-dimensional coupling approaches, the term "equi-dimensional" means that both continua have the same dimensions, such as two-dimensional porous - two-dimensional free-flow systems or three-dimensional porous - three-dimensional free-flow systems. Darcy's Law, which commonly substitutes the momentum equation in the porous-media region, is a first-order differential equation, whereas the momentum equation in the free flow region is in general a second-order differential equation. Thus, porous-media flow equations and free-flow equations are mathematically incompatible at the interface between the domains. In the literature, there are different approaches to overcome this problem. Brinkman suggested to use the same momentum equation for both flow regions [Brinkman (1947)]. Another approach, proposed by Beavers and Joseph, applies an interface condition between the two flow regions which simply relates the gradient of the free-flow velocity to the Darcy velocity in the porous medium [Beavers and Joseph (1967)].

In a lower-dimensional coupling approach, one system - in the present study this is always the free-flow system - has a lower dimension than the other one. If, for example, the free-flow region has a pipe-shaped form, i.e. the length of the pipe is much greater than its diameter, one may reasonably use one-dimensional pipe-flow equations where the velocity along the pipe network is cross-sectionally averaged. In this case, frictional forces can be calculated, for example, using the Darcy-Weisbach friction factor [Darcy (1857), Weisbach (1851)]. In this study, in the free-flow regions only laminar flow conditions are considered.

Lower-dimensional modeling is not new but has been also widely used for the simulation of flow in fractured porous media. The fractures are then implemented as one dimension lower than the dimensions of the porous medium. Reichenberger, Jakobs, Bastian, and Helmig (2006), for example, developed a discrete fracture model, where the flow in the fracture system is described by the parallel plate concept. Bauer, Liedl, and Sauter (2003) used a lower-dimensional dual-continuum coupling technique for single-phase flow to model the karstification of a conduit in a fissured porous medium.

In this study, we extend the dual-continuum concept for coupling multi-phase porous-media flow with lower-dimensional single-phase free flow where different physics in the continua are described by different equations. The focus is to present different new concepts for modelling three-dimensional flow in porous media coupled with one-dimensional pipe flow and to illustrate the characteristic behavior of such systems by numerical test examples. While the equations in each domain are implicitly solved, the coupling of the two flow continua is done explicitly. The coupling strategy is based on a dual-continuum model concept, i.e. two domains lie one on top of each other and mass exchange is calculated by additional source/sink terms.

The manuscript is organised as follows:

After this introduction, the basic concepts and methods used in this study are explained. These include the construction of the geometric features that allow the dual-continuum description of the two domains of different dimensions as well as the explanation of some fundamental equations and the coupling strategy. Furthermore, we give insight into numerical models for specific problem cases and then present and discuss some numerical results showing the characteristic behaviour of the system.

## **2 Basic Model Concept**

### ***2.1 Conservation equations***

The aim of this study is the development of different model concepts for the interaction of multi-phase flow processes in porous media with single-phase free flow in one-dimensional structures. In the following, the conservation equations are considered separately for each system.

#### ***2.1.1 Conservation equations for multi-phase flow in porous media:***

The conservation equations for multi-phase flow in porous media are the mass balance of each component  $k$  in all  $\alpha$  phases (Eq. 1) and the momentum balance of each phase  $\alpha$  (which is in fact an extended version of Darcy's Law for multi-phase

flow (Eq. 2)). The mass balance equation for each component  $k$  comprises a storage term, an advective transport term, a diffusive-dispersive transport term and a source/sink term [Class, Helmig, and Bastian (2002)]. See Appendix A for the nomenclature.

$$\Sigma_{\alpha} \left[ \frac{\partial(\phi \rho_{\alpha} x_{\alpha}^k S_{\alpha})}{\partial t} \right] + \Sigma_{\alpha} \left[ \vec{\nabla} \cdot (\rho_{\alpha} x_{\alpha}^k \vec{u}_{\alpha}) \right] - \Sigma_{\alpha} \left[ \vec{\nabla} \cdot (\vec{D}_{\alpha}^k \nabla(\rho_{\alpha} x_{\alpha}^k)) \right] = q^k \quad (1)$$

$$\vec{u}_{\alpha} = -\frac{k_{r\alpha} \bar{K}}{\mu_{\alpha}} (\nabla p_{\alpha} - \rho_{\alpha} \vec{g}) \quad (2)$$

### 2.1.2 Conservation equations for free flow:

The conservation equations for single-phase free flow include a mass balance equation (Eq. 3) and a momentum balance equation (Eq. 4). The momentum balance equation includes a momentum storage term, a momentum advection term, internal forces due to pressure and viscous forces, and external forces such as gravity.

$$\frac{\partial \rho}{\partial t} + \vec{\nabla} \cdot (\rho \vec{u}) = q \quad (3)$$

$$\frac{\partial(\rho \vec{u})}{\partial t} + \vec{\nabla} \cdot (\rho \vec{u} \otimes \vec{u} + p \vec{I} - \vec{\tau}) = \rho \vec{f}_{ext} \quad (4)$$

### 2.1.3 Conservation equations for a quasi-one-dimensional pipe flow system

The basic assumption in this study for the description of a pipe-flow system is one-dimensional flow behavior. If the free-flow equations (Eq. 3 and Eq. 4) are written for cross-sectionally averaged velocities in 1D flow, one obtains Eq. 5 for the conservation of mass and Eq. 6 for the conservation of momentum. The vector  $\vec{s}$  stands for the unit positive direction of the pipe and  $\tau_w$  is the wall shear stress, which can be approximated by the Darcy-Weisbach approach.

$$\frac{\partial \rho}{\partial t} + \frac{\partial}{\partial s} (\rho u_s) = q \quad (5)$$

$$\frac{\partial(\rho u_s)}{\partial t} + \frac{\partial(\rho u_s u_s)}{\partial s} + \frac{\partial p}{\partial s} + \tau_w \frac{\pi d}{A} = \rho \vec{g} \cdot \vec{s}, \quad (6)$$

, where  $\tau_w = \frac{\lambda}{8} \rho u_s^2$ , and  $\rho = \frac{p}{RT}$ .

The arising system of equations has four unknowns but only two partial differential equations. To close the system, it is assumed that the ideal gas law is valid, i.e. density and pressure are related to each other, and the wall friction is described by the Darcy-Weisbach friction factor ( $\lambda$ ), which is a function of  $f(Re, \frac{\epsilon}{d})$ , where  $Re$  is the Reynolds number,  $\epsilon$  is the roughness of the pipe and  $d$  is the pipe diameter.

## **2.2 Discretization techniques**

For the sake of completeness, a brief overview is given of the discretization methods applied. For further details, the reader is referred to previous publications, e.g. Bastian and Helmig (1999).

For the spatial discretization, a subdomain-collocation finite-volume method (BOX method) is used. The BOX method requires the construction of a secondary mesh. This is achieved by connecting the centers of gravity of the elements with the mid-points of the element edges. Each node is assigned a unique control volume, and each element contains a number of sub-control volumes equal to the number of nodes in that element. The BOX scheme can be derived using the principle of weighted residuals applied on the primary finite element mesh with piece-wise constant weighting functions for the control volumes (boxes) on the secondary mesh. Mass lumping and full upwinding for the advective terms are applied.

The systems of partial differential equations arising from the mathematical description of multi-phase porous-media flow are in general highly non-linear. They are linearized using a damped inexact Newton-Raphson method, as described in Dennis and Schnabel (1996). For the time discretization, a fully-implicit Euler scheme is applied for each particular model.

The flow and transport processes in porous media and free flow are running in different time scales. In general, the free-flow models require smaller time steps and finer grids than the porous-media models, due to the fact that the flow velocities in porous-media regions are much more slower than in pipe-flow regions. For the coupled models, the free flow model (in this case the pipe-flow model) is decisive in determination of the discretization size both in time and in space. We used dual overlapping grids, where both grids are refined along the pipe network. The time-step size is kept the same for both models and it is chosen as small as required by the pipe-flow model.

### **2.2.1 1D pipe-network grid embedded in a 3D porous grid**

The numerical modeling of coupled one-dimensional pipe flow with three-dimensional porous-media flow requires a special grid concept that allows the representation of

interactions between the pipe-network grid and the porous-media grid. Although this is a rather technical issue, it is the basis for the implementation of the model concept and a few explanations are appropriate. The basic idea is to isolate pipe lines within the three-dimensional porous medium grid according to the following concept:

First, a full three-dimensional grid is generated. Then, a "pps" (pipe position) file is created where the positions of the starting and end points of each pipe section, the property identities of sections, and boundary identities of each end point for each pipe section are defined. Fig. 1 shows an exemplary "pps" file structure with 41 pipe sections. The first section starts at point (5, 5, 3.6), ends at point (5, 5, 5), and has the property identifier (ID) 8. The starting point has the boundary ID 99 (denoting an internal boundary) and the end point has the boundary ID 2.

41 #	PIPES	X1,	Y1,	Z1,	X2,	Y2,	Z2,	PIPEPARAMETER1,	BOUNDARYCONDITION [0],	BOUNDARYCONDITION [1],
5	5	3.6	5	5	5	8	99	2		
3.6	5	3.6	5	5	3.6	8	99	99		
3.6	5	2.4	3.6	5	3.6	8	99	99		
2.4	5	2.4	3.6	5	2.4	8	99	99		
4.8	5	2.4	3.6	5	2.4	8	99	99		
4.8	5	0	4.8	5	2.4	8	1	99		
2.4	5	1.2	2.4	5	2.4	8	99	99		
1.2	5	1.2	2.4	5	1.2	8	99	99		
3.6	5	1.2	2.4	5	1.2	8	99	99		
1.2	5	0	1.2	5	1.2	8	1	99		
3.6	5	0	3.6	5	1.2	8	1	99		
6.4	5	3.6	5	5	3.6	8	99	99		
6.4	5	2.4	6.4	5	3.6	8	99	99		
5.2	5	2.4	6.4	5	2.4	8	99	99		
7.6	5	2.4	6.4	5	2.4	8	99	99		
5.2	5	0	5.2	5	2.4	8	1	99		
7.6	5	1.2	7.6	5	2.4	8	99	99		
6.4	5	1.2	7.6	5	1.2	8	99	99		
8.8	5	1.2	7.6	5	1.2	8	99	99		
6.4	5	0	6.4	5	1.2	8	1	99		
8.8	5	0	8.8	5	1.2	8	1	99		
5	3.6	3.6	5	5	3.6	8	99	99		
5	3.6	2.4	5	3.6	3.6	8	99	99		
5	2.4	2.4	5	3.6	2.4	8	99	99		
5	4.8	2.4	5	3.6	2.4	8	99	99		
5	4.8	0	5	4.8	2.4	8	1	99		
5	2.4	1.2	5	2.4	2.4	8	99	99		
5	1.2	1.2	5	2.4	1.2	8	99	99		
5	3.6	1.2	5	2.4	1.2	8	99	99		
5	1.2	0	5	1.2	1.2	8	1	99		
5	3.6	0	5	3.6	1.2	8	1	99		
5	6.4	3.6	5	5	3.6	8	99	99		
5	6.4	2.4	5	6.4	3.6	8	99	99		
5	5.2	2.4	5	6.4	2.4	8	99	99		
5	7.6	2.4	5	6.4	2.4	8	99	99		
5	5.2	0	5	5.2	2.4	8	1	99		
5	7.6	1.2	5	7.6	2.4	8	99	99		
5	6.4	1.2	5	7.6	1.2	8	99	99		
5	8.8	1.2	5	7.6	1.2	8	99	99		
5	6.4	0	5	6.4	1.2	8	1	99		
5	8.8	0	5	8.8	1.2	8	1	99		

Figure 1: pps file format for defining 1D network sections

The models are developed under *DuMur*<sup>x</sup> (multi-scale multi-physics toolbox for the simulation of flow and transport processes in porous media) [Flemisch, Fritz, Helmig, Niessner, and Wohlmuth (2007)], which is based on DUNE (Distributed and Unified Numerics Environment) [Bastian, Blatt, Engwer, Dedner, Klöfkorn, Kuttanikkad, Ohlberger, and Sander (2006)]. DUNE can read grids, for example, in dgf (dune grid format) format. Therefore, a convertor is programmed which combines the 3D grid information with the 1D pipe network information in the dgf file format.

```

6.4000000e+00 4.8000000e+00 4.8000000e+00 0 0 % 43081
6.4000000e+00 4.8000000e+00 5.0000000e+00 0 0 % 43082
6.4000000e+00 5.0000000e+00 0.0000000e+00 8 1 % 43083
6.4000000e+00 5.0000000e+00 2.0000000e-01 8 0 % 43084
6.4000000e+00 5.0000000e+00 4.0000000e-01 8 0 % 43085
6.4000000e+00 5.0000000e+00 6.0000000e-01 8 0 % 43086
6.4000000e+00 5.0000000e+00 8.0000000e-01 8 0 % 43087
6.4000000e+00 5.0000000e+00 1.0000000e+00 8 0 % 43088
6.4000000e+00 5.0000000e+00 1.2000000e+00 8 99 % 43089
6.4000000e+00 5.0000000e+00 1.4000000e+00 0 0 % 43090
6.4000000e+00 5.0000000e+00 1.6000000e+00 0 0 % 43091
6.4000000e+00 5.0000000e+00 1.8000000e+00 0 0 % 43092
6.4000000e+00 5.0000000e+00 2.0000000e+00 0 0 % 43093
6.4000000e+00 5.0000000e+00 2.2000000e+00 0 0 % 43094
6.4000000e+00 5.0000000e+00 2.4000000e+00 8 99 % 43095
6.4000000e+00 5.0000000e+00 2.6000000e+00 8 0 % 43096
6.4000000e+00 5.0000000e+00 2.8000000e+00 8 0 % 43097
6.4000000e+00 5.0000000e+00 3.0000000e+00 8 0 % 43098
6.4000000e+00 5.0000000e+00 3.2000000e+00 8 0 % 43099
6.4000000e+00 5.0000000e+00 3.4000000e+00 8 0 % 43100
6.4000000e+00 5.0000000e+00 3.6000000e+00 8 99 % 43101
6.4000000e+00 5.0000000e+00 3.8000000e+00 0 0 % 43102
    
```

Figure 2: a section of a dgf file format including the 1D network grid information

The generated dgf file includes the 3D grid as well as the boundary identities and the properties of each pipe section. This information is stored for each point belonging to the 1D network grid (see Fig. 2). Fig. 3 shows a resulting 1D network grid embedded in a 3D domain.

The following section gives more details on the strategy for coupling porous-media flow with lower-dimensional pipe flow.

### 2.3 Coupling flow systems of different dimension

The term lower-dimensional coupling in the following means that one flow system has a lower dimension than the other system with which it is coupled. The particular focus of this study is on coupling three-dimensional porous media flow with one-dimensional pipe flow. A major assumption when considering flow in a pipe as

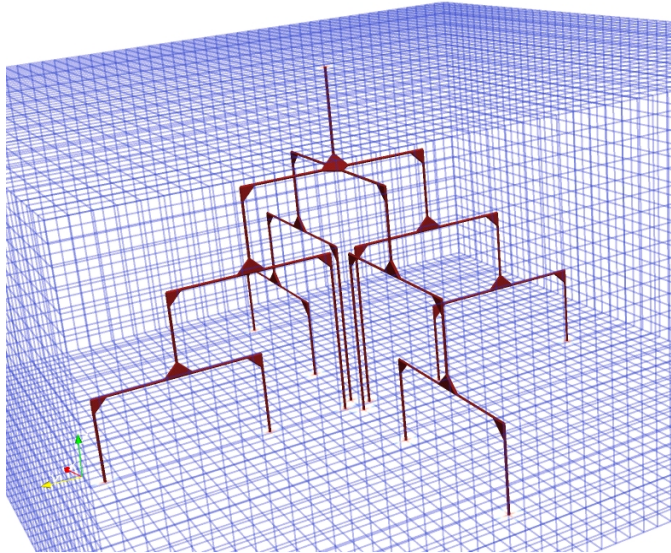


Figure 3: 1D network grid in 3D domain

one-dimensional is that the velocity can be averaged at each cross-section along the pipe, i.e. it is then constant for each cross-section. This assumption severely limits the applicability of coupling schemes available in the literature. For example, the Beavers and Joseph interface condition, which was developed for equi-dimensional coupling, relates the gradient of the free-flow velocity at the interface to the Darcy flow velocity in the porous medium. However, one cannot speak of a velocity gradient perpendicular to the pipe direction in a one-dimensionally averaged pipe-flow model. The use of a dual-continuum coupling strategy is proposed, accounting only for the mass transfer between porous media and pipe flow continua. One could add another exchange term for the momentum transfer between both continua in a dual-continuum model. However, the determination of the momentum exchange rate would require an averaging technique, where the slip boundary condition at the interface should be averaged over the cross-section of the pipe. Eventually, this would introduce another exchange coefficient for the momentum exchange rate, which would not only make the dual-continuum model more complicated but also more uncertain or overparameterized. That kind of approach is beyond the scope of the work we present in this manuscript.



*Dual-continuum coupling*

The dual-continuum model concept for fractured aquifer systems was introduced by Barenblatt, Zheltov, and Kochina (1960) and Warren and Root (1963). Due to the high contrast in properties of fracture system and porous matrix, the total system is realized as two overlapping interacting continua, which occupy the same computational domain. This kind of approach requires homogenization of discrete fracture network parameters (porosity, permeability etc.) for the equivalent representative elementary volumes in fracture continua. Each continuum is modeled by its own conservation equations and the interactions between each continuum are described by an exchange term. In the literature dual-continuum models can be classified as dual-porosity, dual-permeability or multiple interacting continua (MINC). In dual-porosity models, the fracture continua elements are connected to each other and to the elements of matrix continua, whereas the elements of matrix continua are not connected to each other (e.g. Bibby (1981)). This kind of model is suitable for fractured rock systems, where the flow is mainly in the fracture continuum and the rock matrix acts as an additional storage volume. In dual-permeability models the matrix continua are also connected to each other (e.g. Gerke and van Genuchten (1993)). Such models are suitable for fractured matrix systems, where flow occurs both in fracture and in matrix continua. The MINC method is developed by Pruess and Narasimhan (1982). It is basically an extension of the dual-porosity model, where instead of a single matrix continuum several nested matrix continua are introduced to better represent transient flow behaviour.

We developed a dual-continuum model approach similar to the dual-permeability model in the sense that the elements in the porous medium continua are connected to each other. Since the pipe-flow domain is modeled as a discrete pipe-network model with its real geometry, there is no need for homogenization of pipe parameters for the whole domain. Two continua (here: porous medium and pipe network) lie on top of each other and the mass exchange between the continua is calculated by adding an exchange source/sink term (Eq. 7) to the mass conservation equations of both systems with different signs.

$$\int q_{ex} dV = \alpha_{EX} \cdot (p_{pipe} - p_{porous}), \tag{7}$$

where  $\alpha_{EX} = f(\text{fluid properties, pipe geometry, porous media properties})$

$\alpha_{EX}$  is a lumped exchange coefficient which is a function of the hydraulic situation in both domains, the fluid properties, the geometry of the pipe, and the porous media properties. Each model in itself is discretized with an implicit first order backward Euler method in time. The coupling strategy with respect to the exchange

terms can be considered as being explicit. In a kind of pseudo-algorithmic manner, the explicit coupling strategy may be described as follows:

- initialize the pressure in the porous medium and solve the porous medium flow problem;
- set the porous-medium pressure  $p_{porous}$  to calculate the mass exchange term to be applied to the pipe-flow problem;
- solve the pipe-flow problem;
- set the pipe pressure  $p_{pipe}$  for calculating the mass exchange term to be applied in the porous-medium flow problem;
- solve the porous-medium flow problem;
- iterate until it converges.

### 3 Dual-continuum models via lower-dimensional coupling: Example applications

This section provides a couple of applications of the different models in order to illustrate the characteristic behaviors of the modeled systems. The chosen sequence of example applications follows the order of increasing complexity of the applied model concepts.

#### 3.1 Coupling single-phase flow in porous media with Hagen-Poiseuille free flow

As a first step, the numerical implementation is done for a very simplified system, i.e. steady-state incompressible flow.

The multi-phase mass balance equation (Eq. 1) simplifies to Eq. 8 and Darcy's Law (Eq. 9) holds for single-phase porous-media flow:

$$\vec{\nabla} \cdot (\rho \vec{u}) = q + \boxed{q_{ex}}, \text{ where } q_{ex} \text{ is the mass exchange term} \quad (8)$$

$$\vec{u} = -\frac{\bar{K}}{\mu} (\nabla p - \rho \vec{g}) \quad (9)$$

The mass balance equation of pipe flow (Eq. 10) has the same mass exchange term as the porous media mass balance equation, but with a different sign. If the momentum storage and the momentum inertia terms are smaller than the viscous term

and the flow conditions are laminar, then the free-flow momentum equation (Eq. 6) can be simplified to the well-known Hagen-Poiseuille equation (Eq. 13):

$$\frac{\partial}{\partial s}(\rho u_s) = q - \boxed{q_{ex}} \quad (10)$$

$$\tau_w \frac{\pi d}{A} = -\frac{\partial p}{\partial s} + \rho \vec{g} \cdot \vec{s} \quad (11)$$

$$\tau_w = \frac{\lambda}{8} \rho u_s^2, \text{ for laminar flow } \lambda = \frac{64}{Re}, \lambda = \frac{64\nu}{u_s d} \quad (12)$$

$$\tau_w = \frac{8 u_s \nu \rho}{d} \Rightarrow \text{insert in Eq. 11 we get } \frac{32 u_s \nu \rho}{d^2} = -\frac{\partial p}{\partial s} + \rho \vec{g} \cdot \vec{s} \quad (13)$$

For the calculation of the mass exchange term (Eq. 14), one has to take into account the fluid properties (density( $\rho$ ) and dynamic viscosity ( $\mu$ )), the porous-media properties (the exchange coefficient ( $\alpha_{ex}$ )), the pipe geometry (the outer surface of the pipe element ( $A_{outerface}$ ) and the pipe diameter ( $d$ )), and the pressure difference between the two systems:

$$\int q_{ex} dV = \rho \frac{\alpha_{ex}}{\mu} \frac{A_{outerface}}{d} (p_{pipe} - p_{porous}) \quad (14)$$

*The test problem for coupling porous media with single pipe:*

A problem is set up where a pipe with a diameter of 2 cm passes through the porous medium from left to right and flowing fluid is water. The porous domain is 2 m high, 2 m wide and 10 m long. In this example, gravity is set to zero in order to see the effect of the exchange term clearly. At the left and right boundaries of the porous domain, Dirichlet boundaries are set to  $p_{left} = 1.004$  bar and  $p_{right} = 1.0$  bar. The permeability of the porous medium is  $5.0 \cdot 10^{-10}$  m<sup>2</sup>. At the left boundary of the pipe, a no-flow boundary is set and at the right boundary, the pressure is fixed at 1.0 bar. The exchange coefficient is chosen as  $1.2 \cdot 10^{-11}$  m<sup>2</sup> (see Fig. 4).

The left figure in Fig. 5 shows the steady state pressure distribution along the pipe for both porous medium and pipe flow. The right side of the same figure shows the

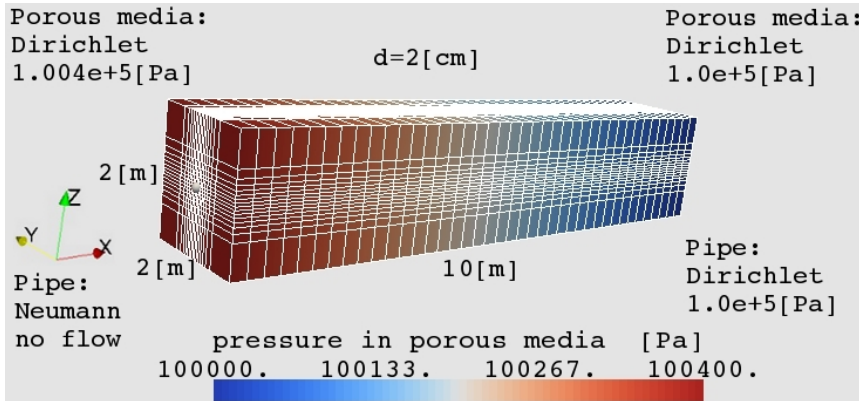


Figure 4: Coupled porous-media flow - pipe-flow problem

velocity distribution along the pipe. To examine the effect of coupled flow on the porous medium pressure distribution, a cut plane at  $y = 1$  m is shown in Fig. 6. If there was no coupled flow, one would expect to see a linear pressure distribution in the porous medium since the flow is incompressible. However, the figure clearly shows that the pressure isolines are not linear, thus indicating the influence of the pipe-flow coupling on the hydraulics in the porous medium.

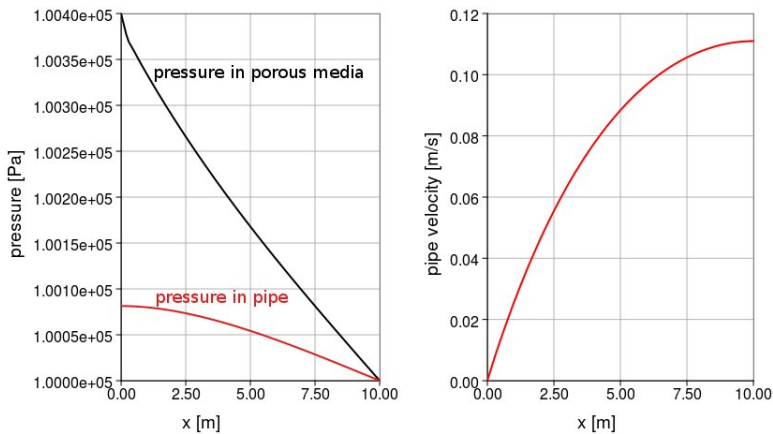


Figure 5: Pressure and velocity distribution along the pipe

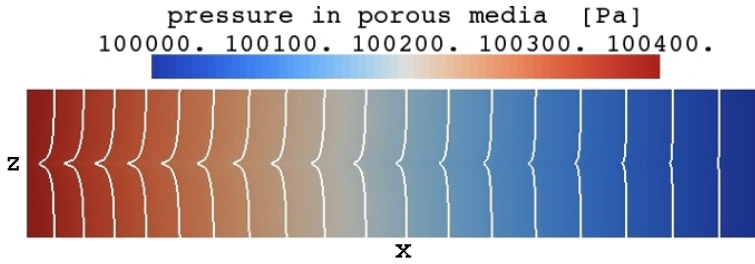


Figure 6: Pressure distribution in a cut plane at  $y = 1$  [m] in the porous medium

*The test problem for coupling porous media with pipe network:*

Another problem is simulated where a pipe network passes through a porous medium and flowing fluid is water (Fig. 3). As in the first example, gravity is again neglected. The porous medium has a rectangular prism shape with  $x = 10$  m,  $y = 10$  m and  $z = 5$  m. All pipes have a diameter of 2 cm. The boundary conditions for this system are as follows: The sides of the porous domain are no-flow Neumann boundaries, whereas the top boundary is set to a constant pressure of 1.004 bar and at the bottom boundary, the pressure is set to 1.0 bar. The pipe-network system has a no-flow boundary at the top and a fixed pressure of 1.0 bar at the bottom. The permeability of the porous medium is  $5.0 \cdot 10^{-10}$  m<sup>2</sup> and the exchange coefficient is chosen as  $1.2 \cdot 10^{-11}$  m<sup>2</sup>. Fig. 7 shows the porous-medium pressure distribution. The gradients of the pressure isolines show clearly that there is a considerable flow from the porous medium into the pipe-network system, which could be described by the model.

**3.2 Coupling compressible single-phase flow in porous media with compressible single-phase pipe flow**

In the next step, the numerical models are extended for transient compressible flow conditions.

The conservation equations for compressible one-phase flow in porous media can be written as:

$$\frac{\partial(\phi\rho)}{\partial t} + \vec{\nabla} \cdot (\rho\vec{u}) = q + \boxed{q_{ex}} \tag{15}$$

,where  $q_{ex}$  is the mass exchange term, and  $\rho = \frac{p}{RT}$  .

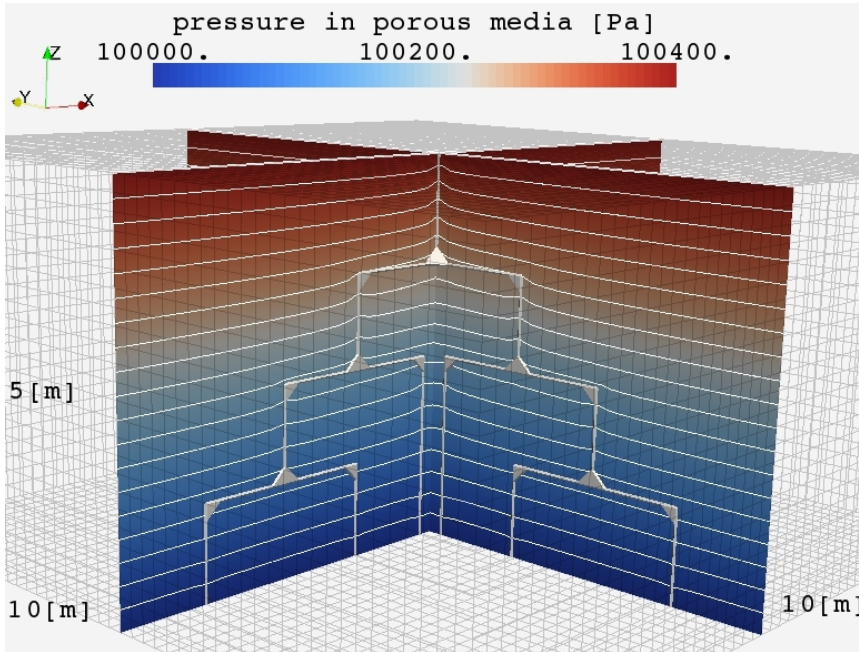


Figure 7: Pressure distribution in the porous medium for a coupled porous medium - pipe-network system

$$\vec{u} = -\frac{\bar{K}}{\mu}(\nabla p - \rho \vec{g}) \quad (16)$$

The conservation equations for the pipe flow are:

$$\frac{\partial \rho}{\partial t} + \frac{\partial}{\partial s}(\rho u_s) = q - \boxed{q_{ex}} \quad (17)$$

$$\frac{\partial(\rho u_s)}{\partial t} + \frac{\partial(\rho u_s u_s)}{\partial s} + \frac{\partial p}{\partial s} + \tau_w \frac{\pi d}{A} = \rho \vec{g} \cdot \vec{s} \quad (18)$$

Exchange term:

$$\int q_{ex} dV = \rho_{ex} \frac{\alpha_{ex} A_{outerface}}{\mu d} (p_{pipe} - p_{porous}) \quad (19)$$

Because density depends on pressure changes for compressible flows,  $\rho_{ex}$  in the mass exchange term needs to be determined. The density exchange term is up-winded, i.e. if  $p_{pipe} < p_{porous} \Rightarrow \rho_{ex} = \rho_{porous}$ , else  $\rho_{ex} = \rho_{pipe}$ .

The test problem for coupling porous media with single pipe

A test problem is set up as described in the upper part of Fig. 8 and the flowing fluid is air. In the same figure the lower left and lower right parts show the pressure distributions in both domains. The difference between this test problem and the test problem in Fig. 4 lies in the flowing fluid. The boundary conditions are the same as before, but this time air is flowing instead of water. If we compare the left part of Fig. 5 with the lower left part of Fig. 8, we can see that the pressure difference is higher in the second case. This doesn't necessarily mean that the mass exchange rate is higher in the second case because it also depends on the kinematic viscosity of the fluid ( $1/\nu = 1/(\mu/\rho)$ ). Although the same boundary conditions are set for both problem cases, they are not directly comparable to each other. Different amounts of mass are stored in each problem depending on the fluid properties, and the governing equations for both problems are not identical. However, we will compare and discuss the problem given in Fig. 8 further in section 3.4 where the coupling of two-phase porous-media flow with single-phase pipe flow is presented.

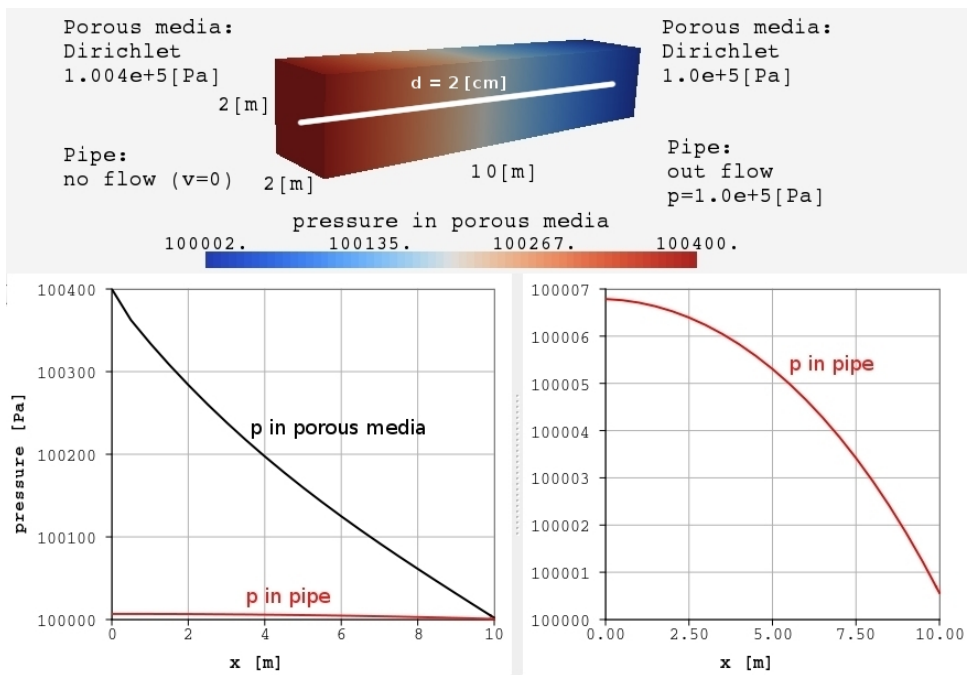


Figure 8: Boundary conditions and pressure distribution for a coupled porous medium - one-phase pipe flow

### 3.3 Richard's equation - Hagen Poiseuille coupling

The coupling of the Richard's equation in the porous medium with the Hagen-Poiseuille equation in the pipe is implemented as an intermediate step towards considering multi-phase flow in the porous medium. This increase in complexity compared with the previous example allows us to show the influence of capillary effects in the porous domain during the dual-continuum coupling. Such a flow system could become relevant, for example, in a macropore flow problem. Water flows relatively fast in so-called macropore structures like root channels or worm-holes, and there is an exchange of water between the macropores (the pipes) and the unsaturated zone (the porous medium), where capillary effects are important.

The unsaturated soil zone can be modeled with a two-phase flow model where the fluid phases are water and air. The presence of gas in the soil causes some additional resistance for the water flow in porous media. However, the dynamic viscosity of air is only about 2% of the viscosity of water, making the gas phase highly mobile. Therefore, a simplified approach for the two-phase flow problem could be a reduction of the multiphase flow equation to Richard's problem [Richards (1931)] where the mobility of the gas phase is assumed to be infinite. Richard's equation not only considers the water phase but also capillary effects, where the pressure of the gas phase is set to a reference pressure ( $p_{nref}$ ):

$$\rho \phi \frac{\partial S_w}{\partial p_c} \frac{\partial p_c}{\partial t} - \vec{\nabla} \cdot \left( \frac{k_{rw}}{\mu_w} \rho_w K (\nabla p_w - \rho_w \vec{g}) \right) = q + \boxed{q_{ex}}, \tag{20}$$

,where  $p_w = p_{nref} - p_c$  and  $p_{nref} = 100000$  Pa.

The macropores are modeled with the Hagen-Poiseuille formulation (from Eq. 10 to Eq. 13).

In contrast to the single-phase flow coupling, the exchange term here (Eq. 21) includes a mobility exchange term ( $\lambda_{ex}$ ) to account for the relative permeability of water in the unsaturated zone (Eq. 21):

$$\int q_{ex} dV = \rho \lambda_{ex} \alpha_{ex} \frac{A_{outerface}}{d} (p_{pipe} - p_{wporous}) \tag{21}$$

The mobility exchange term is upwinded, i.e. if  $p_{pipe} < p_{porous} \Rightarrow \lambda_{ex} = \frac{k_{rw}}{\mu}$ , else  $\lambda_{ex} = \frac{1}{\mu}$ .



*The test problem for coupling porous media with four pipes*

A numerical experiment is set up where four unconnected macropores pass through a porous medium and flowing fluid is water (see Fig. 9). Analogously to the previous examples, gravity is again set to zero. The porous medium has the shape of a cube with sides  $x = y = z = 1.2$  m. The macropores have a diameter of 1 cm. The porous medium is initially unsaturated and the macropores are full of water. The boundary conditions for the system are as follows: the sides of the porous domain are unsaturated, whereas the top and the bottom boundaries are set to a no-flow condition. The macropores have a fixed pressure of 1.0 bar at the top and at the bottom boundaries (see Fig. 9). The permeability of the porous medium is  $5.0 \cdot 10^{-10}$  m<sup>2</sup> and the exchange coefficient is chosen to be the same as the permeability.

In Fig. 10, the top figure shows the saturation distribution after 11 seconds. The bottom figure shows the pressure distribution along the pipes. After 11 seconds, saturation around the macropores increases from 0 to 0.6 and water pressure in the unsaturated zone increases accordingly, whereas macropore pressure decreases. After 5 minutes, as the unsaturated zone fills with water, the capillary pressure in porous media has decreased and the pressure difference between macropore and porous medium has decreased also (see Fig. 11). This means that the discharge from the macropore to the unsaturated zone decreases according to the smaller pressure difference between the two continua.

**3.4 Coupling of two-phase porous-media flow with single-phase pipe flow**

The example application presented in the following is motivated by gas migration in abandoned coal mines. The coal seams in the mines contain adsorbed methane gas. However, the methane desorbs from the coal seams as a result of the sinking pressure during and after mining activity. Methane accumulates in the gas phase of the porous rock or soil and then migrates to the surface through the rocks, but also through the shafts and tunnels of the old mine. Methane emissions to the surface need to be controlled to ensure safe living conditions, since it is suffocative and explosive. If the coal mine is not flooded with groundwater, the surroundings of the tunnels and of the shafts are relatively dry. Given such a case, the methane-migration problem could be modeled as a two-phase porous media flow coupled with a single-phase pipe flow. The main assumption in this model concept is that the mass transfer between the porous medium and the pipe flow only takes place via the gas phase and that the water phase is assumed to stay in the porous medium (see Fig. 12). The conservation equations for two-phase flow in porous media can

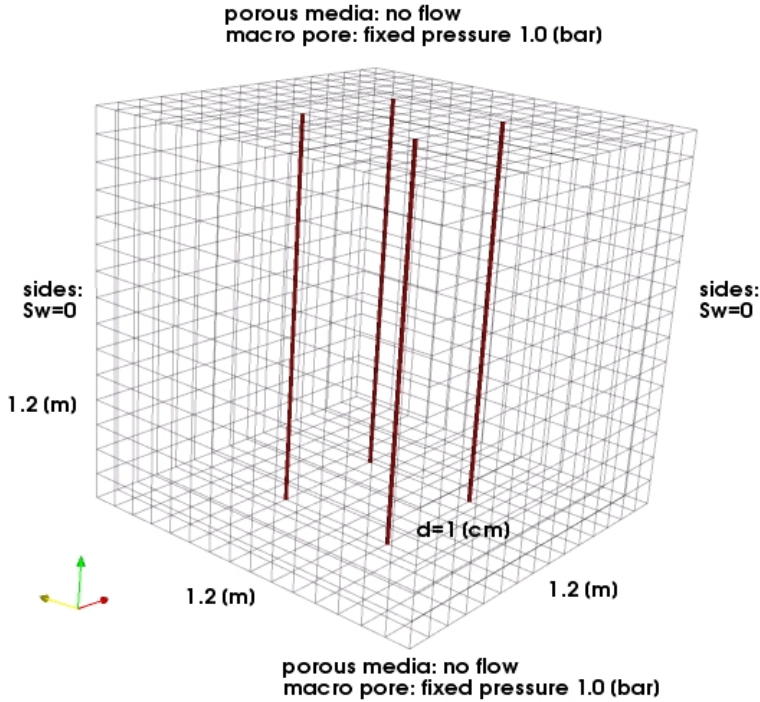


Figure 9: Coupled Richards - macropore problem

be written for the gas phase ( $g$ ) as:

$$\frac{\partial(\phi S_g \rho_g)}{\partial t} - \vec{\nabla} \cdot \left( \rho_g \frac{k_{rg}}{\mu_g} \bar{\bar{K}} \cdot (\nabla p_g - \rho_g \vec{g}) \right) = q_g + \boxed{q_{ex}} \quad (22)$$

and for the water phase ( $w$ ) as:

$$\frac{\partial(\phi S_w \rho_w)}{\partial t} - \vec{\nabla} \cdot \left( \rho_w \frac{k_{rw}}{\mu_w} \bar{\bar{K}} \cdot (\nabla p_w - \rho_w \vec{g}) \right) = q_w \quad (23)$$

The conservation equations for the pipe flow are:

$$\frac{\partial \rho}{\partial t} + \frac{\partial}{\partial s} (\rho u_s) = q - \boxed{q_{ex}} \quad (24)$$

$$\frac{\partial(\rho u_s)}{\partial t} + \frac{\partial(\rho u_s u_s)}{\partial s} + \frac{\partial p}{\partial s} + \tau_w \frac{\pi d}{A} = \rho \vec{g} \cdot \vec{s} \quad (25)$$

The exchange term includes a mobility term ( $\lambda_{ex}$ ) to account for the relative permeability of gas in the unsaturated zone (Eq. 26).

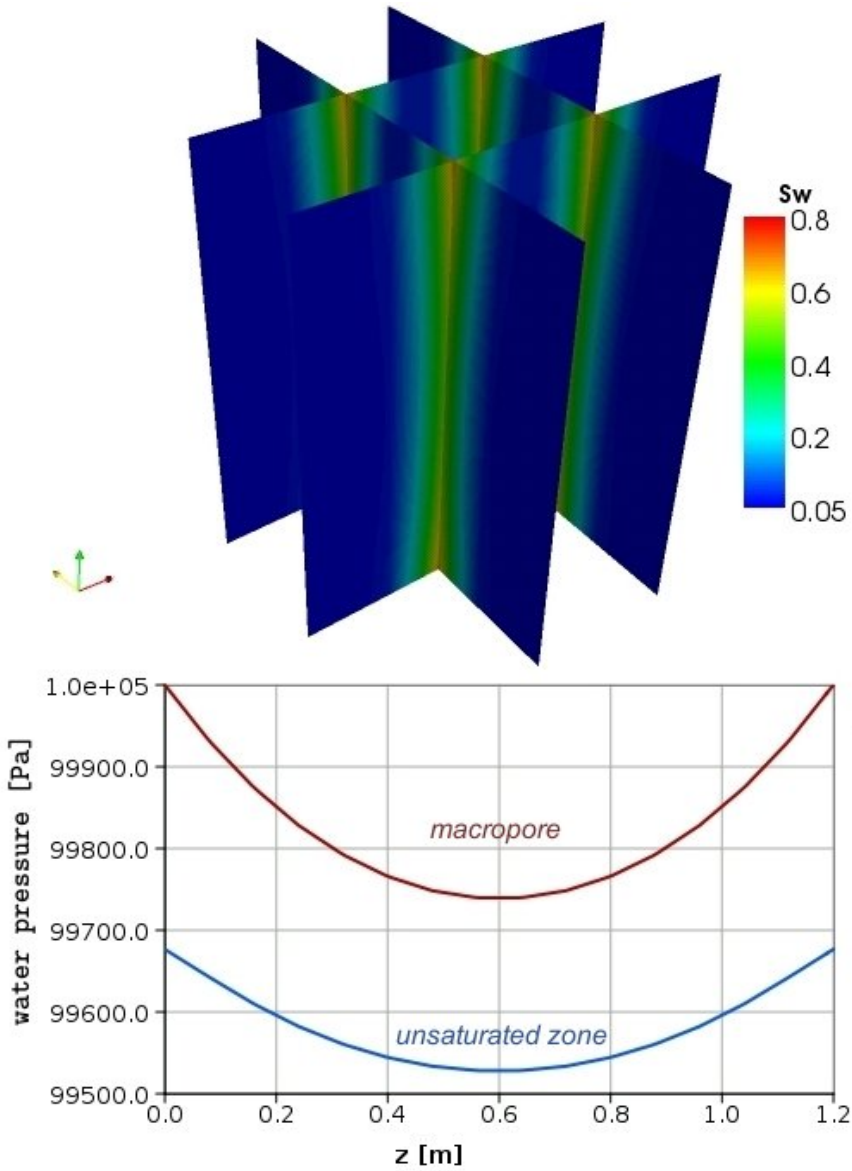


Figure 10: Saturation distribution and pressure distributions after  $t=11$  seconds

Exchange term:

$$\int q_{ex} dV = \rho_{ex} \lambda_{ex} \alpha_{ex} \frac{A_{outerface}}{d} (p_{pipe} - p_{g_{porous}}) \quad (26)$$

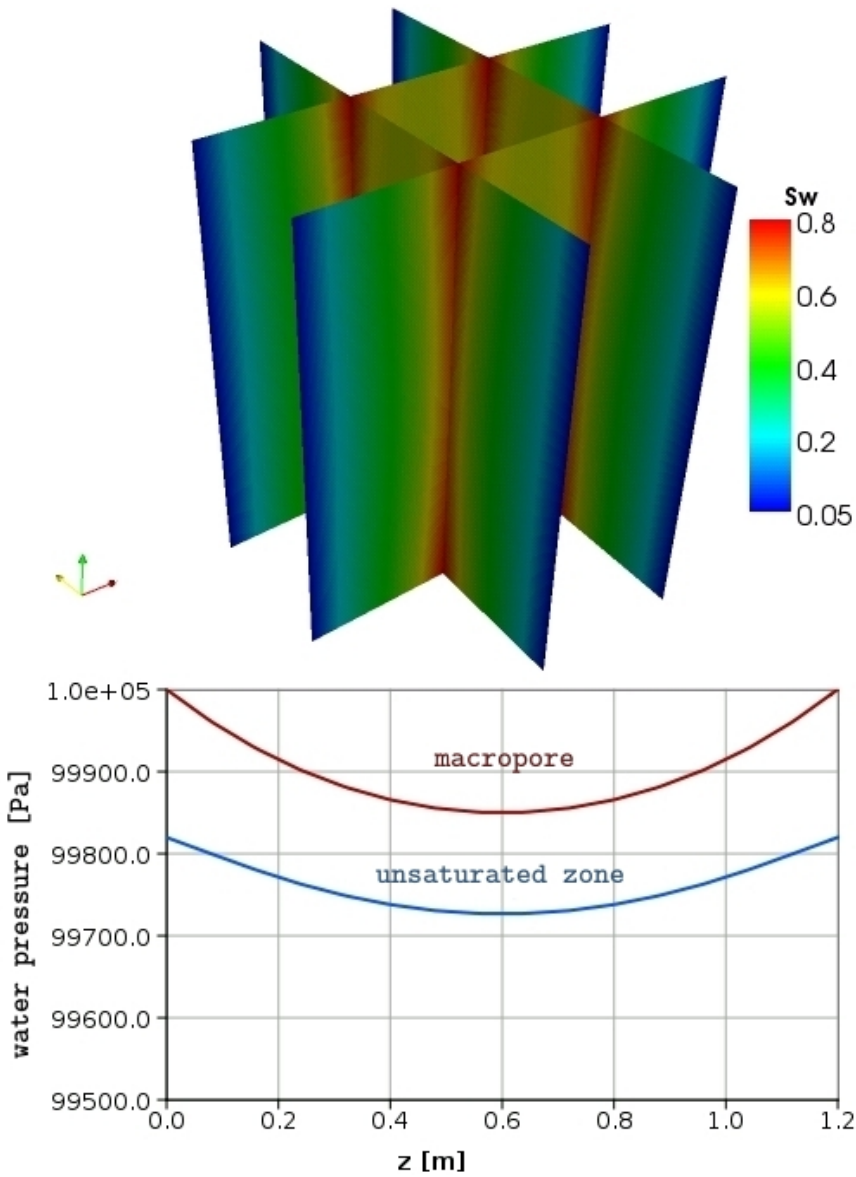


Figure 11: Saturation distribution and pressure distributions after  $t=5$  minutes

Density exchange ( $\rho_{ex}$ ) and mobility exchange ( $\lambda_{ex}$ ) terms are upwinded, i.e.

$$\text{if } p_{pipe} < p_{porous} \Rightarrow \rho_{ex} \cdot \lambda_{ex} = \rho_{porous} \cdot \frac{k_{rgporous}}{\mu}, \text{ else } \rho_{ex} \cdot \lambda_{ex} = \rho_{pipe} \cdot \frac{1}{\mu}.$$

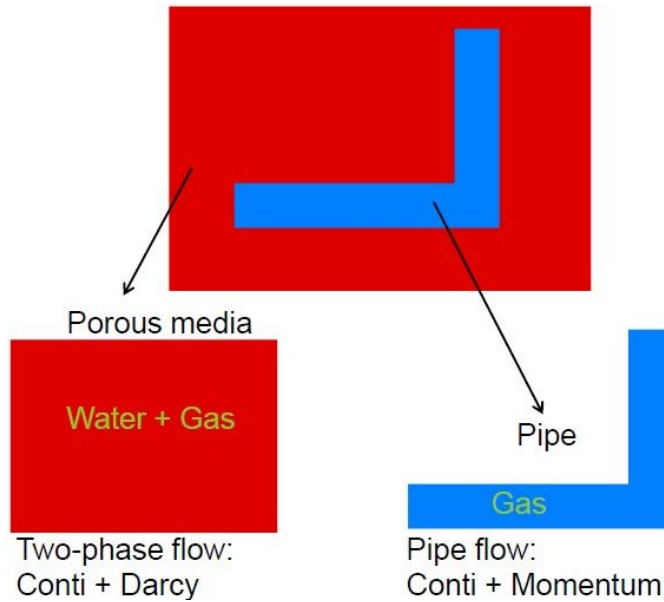


Figure 12: Dual-continuum coupling strategy in two-phase porous-media flow - one-phase pipe-flow systems

*Two test problems for coupling porous media with single pipe:*

Two numerical problems (setup A and setup B) are simulated to see the effects of the mobility-dependent exchange term on the coupled two-phase porous media flow (water and air) - single-phase pipe flow (air) problem (Fig. 13). The same geometric setup as in the single-pipe examples is being used. The pipe has a no-flow boundary condition at the left boundary and a fixed pressure of 1.0 bar at the right boundary. The exchange coefficient is chosen as  $1.2 \cdot 10^{-11} \text{ m}^2$ . In both setups the porous media domain is initially unsaturated and at the right boundary, the saturation of the water phase  $S_w$  is set to 0, while the pressure of the gas phase is fixed at 1.0 bar. In setup A, the saturation of the water phase  $S_w$  is set to 0 at the left boundary of the porous medium, and the pressure of the gas phase is fixed at 1.004 bar. In setup B, the saturation of the water phase  $S_w$  is set to 0.9 at the left boundary of the porous medium. This means that in setup B the porous medium is flooded with water, while in setup A the model should behave like a single-phase system.

Because the boundary conditions, the geometry, and the flowing fluid (air) in setup A are the same as in the problem setup described in the upper part of Fig. 8, both problems are comparable to each other. The pressure distributions in the lower

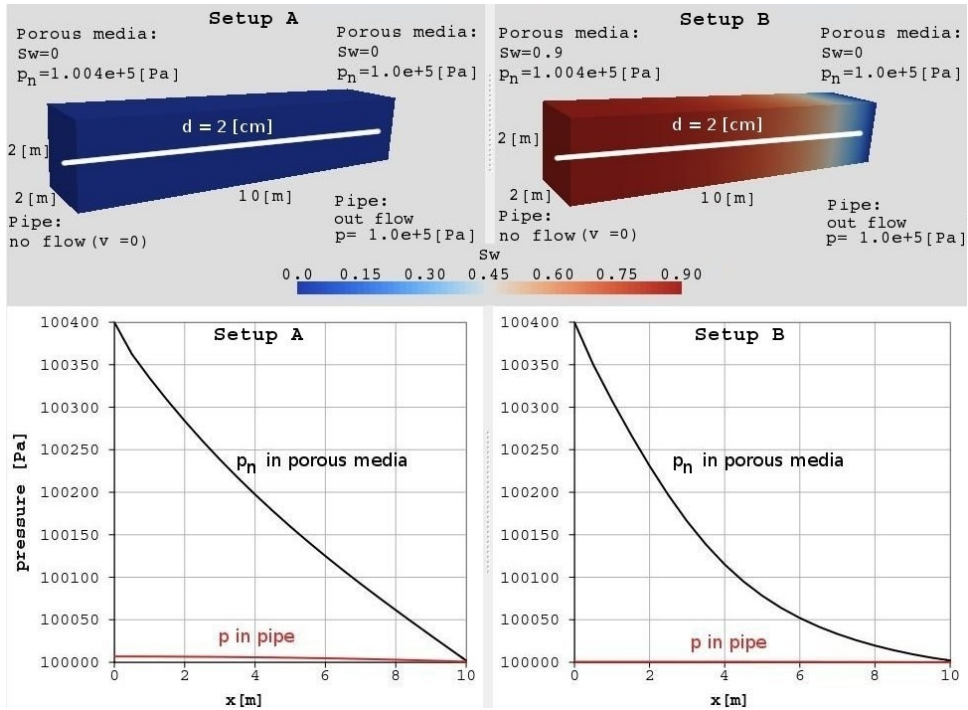


Figure 13: two-phase porous media flow - single-phase pipe flow dual-continuum coupling problem

left part of Fig. 8 are the same as the pressure distribution in the lower left part of Fig. 13. The pipe pressure in setup A (upper curve in Fig. 14) and in the lower right part of Fig. 8 matches well with each other. This comparison clearly shows that, as expected of course, setup A behaves exactly like a single phase system.

In setup B, the porous medium is flooded with water due to the left boundary condition ( $S_w = 0.9$ ). If the steady state pressure distributions along the pipe line for both setups are compared to each other, it can be clearly recognized that the pressure gradient in setup B is lower than the one in setup A, which is a clear hint that less gas is flowing into the pipe when the domain is flooded with water (Fig. 14). The model is capable of representing this effect mainly due to the mobility exchange term ( $\lambda_{ex} = k_{rgporous}/\mu$ ). In setup A, the relative permeability of the gas phase in the porous medium is 1.0. On the contrary, the relative permeability of the gas phase in setup B is only around 0.1. Therefore, at steady state the mobility exchange term in setup A is approximately 10 times larger than in setup B.

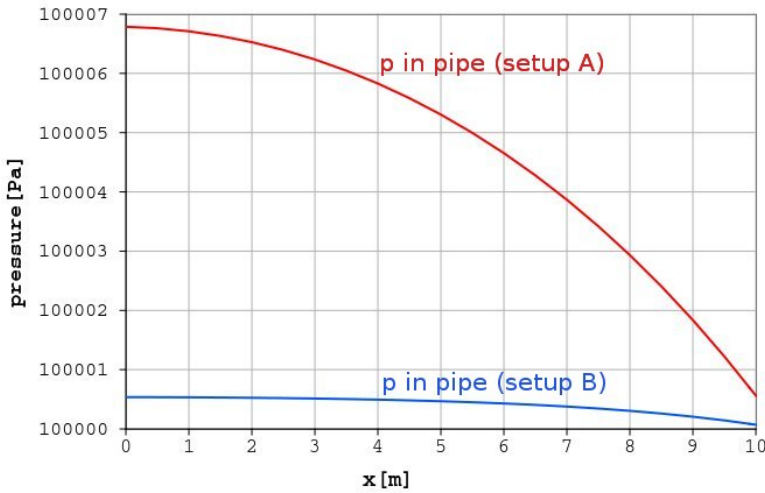


Figure 14: Comparison of pressure distributions in the pipe for setups A and B

#### 4 Summary and Final Remarks

The aim of this study is the development of different model concepts for the interaction of multi-phase flow processes in porous media with single-phase free flow in quasi-one-dimensional structures. This is achieved on the basis of a dual-continuum coupling strategy where the interaction between the flow continua is restricted to mass transfers only. The flow velocity along the pipe network is cross-sectionally averaged, i.e. there is no finite velocity gradient perpendicular to the pipe direction which would be required in order to implement coupling approaches as, for example, suggested by Beavers and Joseph (1967). Although the dual-continuum coupling strategy is easy to implement, it reveals difficulties in the determination of the exchange coefficient ( $\alpha_{ex}$ ).

A series of numerical examples was presented. For the coupling of single-phase porous-media flow with (also single-phase) Hagen-Poiseuille flow in the pipe, it could be shown that the mutual influence of the coupled flow systems on the pressure distribution in both systems can be clearly represented with the dual-continuum coupling strategy. It could also be shown that a geometrically complex pipe-network flow system could be successfully coupled with porous-media flow via the dual-continuum approach. The coupling of Richard's equation in the porous medium with Hagen-Poiseuille flow indicated that capillary forces in the unsaturated zone play the decisive role in the determination of the exchange rate. The study of coupled two-phase porous-media flow with single-phase pipe flow re-

vealed that the mobility exchange term ( $\lambda_{ex}$ ) is a key term in the model since it significantly affects the mass exchange rate between the two continua.

The coupling concepts presented do not comprise all the physical problems that were mentioned in the introduction. The presented examples were kept as simple as possible to show the basic features and characteristics of the model concepts that address processes of different complexity. For this reason, there is not much reference of these examples to real world applications. Flow and transport systems as in fuel cells or cancer therapy need to be modeled by a coupling of the two-phase two-component porous media flow model with single-phase two-component pipe flow model since the transport of the components, for example oxygen or the therapeutic agent respectively, in both media are significant. While the concepts described in this manuscript are presently restricted to pure flow problems, they have to be extended by an additional consideration of transport equations. Yet the present study contributes towards improving the dual-continuum coupling approach also for transport dominated systems, where from the coupling perspective the only difference lies in the number of exchange terms.

## References

- Barenblatt, G. I.; Zheltov, I. P.; Kochina, I. N.** (1960): Basic concepts in the theory of seepage of homogeneous liquids in fissured rocks. *J. Appl. Math. Mech. (Engl. Transl)*, vol. 24, pp. 1286 – 1303.
- Bastian, P.; Blatt, M.; Engwer, C.; Dedner, A.; Klöfkorn, R.; Kuttanikkad, S. P.; Ohlberger, M.; Sander, O.** (2006): The distributed and unified numerics environment (dune). In *Proc. of 19th Symposium on Simulation Technique in Hannover*.
- Bastian, P.; Helmig, R.** (1999): Efficient fully-coupled solution techniques for two phase flow in porous media. Parallel multigrid solution and large scale computations. *Advances in Water Resources*, vol. 23, pp. 199–216.
- Bauer, S.; Liedl, R.; Sauter, M.** (2003): Modeling of karst aquifer genesis: Influence of exchange flow. *Water Resour. Res.*, vol. 39, no. 10.
- Beavers, G. S.; Joseph, D. D.** (1967): Boundary conditions at a naturally permeable wall. *Journal of Fluidmechanics*, vol. 30, pp. 197–207.
- Bibby, R.** (1981): Mass Transport of Solutes in Dual-Porosity Media. *Water Resources Research*, vol. 17, pp. 1075–1081.
- Brinkman, H. C.** (1947): A calculation of the viscous force exerted by a flowing fluid on a dense swarm of particles. *Appl. Sci. Res.*, vol. A1, pp. 27–34.



**Class, H.; Helmig, R.; Bastian, P.** (2002): Numerical simulation of nonisothermal multiphase multicomponent processes in porous media, 1. An efficient solution technique. *Advances in Water Resources*, vol. 25, pp. 533–550.

**Darcy, H. P. G.** (1856): *Les Fontaines Publiques de la Ville de Dijon*. Victor Dalmont.

**Darcy, H. P. G.** (1857): *Recherches expérimentales relatives au mouvement de l'eau dans les tuyaux*. Imprimerie Impériale.

**Dennis, J. E.; Schnabel, R. B.** (1996): *Numerical methods for unconstrained optimization and nonlinear equations*. Society for Industrial and Applied Mathematics (SIAM), Philadelphia, PA.

**Flemisch, B.; Fritz, J.; Helmig, R.; Niessner, J.; Wohlmuth, B. I.** (2007): Dumux: a multi-scale multi-physics toolbox for flow and transport processes in porous media. In *ECCOMAS Thematic Conference on Multi-scale Computational Methods for Solids and Fluids in Paris*.

**Gerke, H.; van Genuchten, M.** (1993): A dual-porosity model for simulating the preferential movement of water and solutes in structured porous media. *Water Resources Research*, vol. 29, pp. 305–319.

**Pruess, K.; Narasimhan, T. N.** (1982): A practical method for modeling fluid and heat flow in fractured media. *Society of Petroleum Engineers*, vol. 25, pp. 14–26.

**Reichenberger, V.; Jakobs, H.; Bastian, P.; Helmig, R.** (2006): A mixed-dimensional finite volume method for two-phase flow in fractured porous media. *Advances in Water Resources*, vol. 29, pp. 1020 – 1036.

**Richards, L.** (1931): Capillary conduction of liquids through porous mediums. *Physics*, pp. 318–333.

**Warren, J. E.; Root, P. J.** (1963): The behaviour of naturally fractured reservoir. *Soc. Petrol. Eng. J.*, vol. 3, pp. 245 – 255.

**Weisbach, J.** (1851): *Lehrbuch der Ingenieur-und Maschinen-Mechanik*. Friedrich Bieweg und Sohn.

**Appendix A: Nomenclature**

The following table shows the symbols used in this paper.

<b>Symbol</b>	<b>Meaning</b>	<b>Dimension</b>
$A$	cross-sectional area of pipe	$[m^2]$
$A_{outerface}$	circumference area of a pipe element	$[m^2]$
$\bar{\bar{D}}$	diffusion coefficient tensor	$[m^2/s]$
$d$	pipe diameter	$[m]$
$\vec{f}_{ext}$	external force tensor per unit mass	$[m/s^2]$
$\vec{g}$	gravitational acceleration	$[m/s^2]$
$\bar{\bar{I}}$	unit tensor	$[-]$
$k_r$	relative permeability	$[-]$
$\bar{\bar{K}}$	permeability tensor	$[m^2]$
$p$	pressure	$[N/m^2]$
$p_n$	non-wetting phase pressure	$[N/m^2]$
$p_{nref}$	reference non-wetting phase pressure	$[N/m^2]$
$p_w$	wetting phase pressure	$[N/m^2]$
$p_c$	capillary pressure	$[N/m^2]$
$q$	source/sink term	$[kg/(m^3 \cdot s)]$
$q_{ex}$	mass exchange term	$[kg/(m^3 \cdot s)]$
$R$	individual gas constant	$[J/(kg \cdot K)]$
$R_e$	Reynold's number	$[-]$
$S$	saturation	$[-]$
$S_w$	wetting phase saturation	$[-]$
$S_n$	non-wetting phase saturation	$[-]$
$\vec{s}$	unit positive direction vector of the pipe	$[-]$
$t$	time	$[s]$
$T$	temperature	$[K]$
$\vec{u}$	velocity vector	$[m/s]$
$u_s$	velocity along the positive pipe direction	$[m/s]$
$V$	volume	$[m^3]$
$x_\alpha^k$	mass fraction of a component $k$ in phase $\alpha$	$[-]$
$\phi$	porosity	$[-]$
$\rho$	density	$[kg/m^3]$
$\bar{\bar{\tau}}$	shear stress tensor	$[Pa]$
$\tau_w$	wall shear stress	$[Pa]$
$\lambda$	Darcy-Weisbach friction factor	$[-]$
$\varepsilon$	equivalent sand grain roughness	$[m]$

$\alpha_{EX}$	lumped exchange coefficient	[m·s]
$\alpha_{ex}$	exchange coefficient	[m <sup>2</sup> ]
$\mu$	dynamic viscosity	[kg/(m·s)]
$\nu$	kinematic viscosity	[m <sup>2</sup> /s]

**subscripts**

ex	exchange
EX	lumped exchange
g	gas phase
n	non-wetting phase
ref	reference
s	along the pipe direction
w	water phase
$\alpha$	phase

**superscripts**

k	component
---	-----------

